Uncovering novel substrates for Aurora A kinase

Teresa Sardon[1,*], Roland A. Pache[2,*], Amelie Stein[2,*], Henrik Molina[1], Isabelle Vernos[1,3,†] and Patrick Aloy[2,3,†]

1. Centre for Genomic Regulation. c/ Dr Aiguader 88, 08003 Barcelona, Spain.

2. Institute for Research in Biomedicine. c/ Baldiri i Reixac 10-12, 08028 Barcelona, Spain.

3. Institució Catalana de Recerca i Estudis Avançats

*These authors contributed equally to this work.

†Corresponding authors:
Isabelle Vernos. Tel: +34 933160275; Email: isabelle.vernos@crg.es
Patrick Aloy. Tel: +34 934039690; Email: patrick.aloy@irbbarcelona.org

Supplementary Information

Set of human protein sequences and interactions

We collected a comprehensive set of human protein sequences by integrating the 17,317 human proteins from UniProtKB/Swiss-Prot, the 54,362 human protein sequences stored in UniProtKB/TrEMBL and the 11,013 annotated human splice variants associated with those UniProt entries (UniProt-Consortium, 2008). This resulted in a non-redundant set of 77,683 human protein sequences. To check for direct and indirect interactions (i.e. mediated by one additional protein) between AurA and the known substrates, as well as between AurA and the 308 spindle proteins, we assembled a human interactome by integrating all human protein-protein interactions reported in IntAct (Kerrien et al., 2007), MINT (Chatr-aryamontri et al., 2007) and HPRD (Mishra et al., 2006), resulting in a non-redundant set of 48,356 interactions among 11,074 proteins.

Motif assessment and derivation

We used M-Coffee (Wallace et al., 2006) to align the known phosphorylation sites identified in our literature search. We assessed the AurA consensus motifs found in the literature using the alignment of the phosphorylation site ±10 residues and derived the notP motif by comparing conserved and non-conserved positions.

List of spindle proteins

We extracted the lists of proteins whose localization to the centrosome, the spindle apparatus or the kinetochores was known and/or has been confirmed through the large-scale proteomics studies conducted by Andersen *et al.* (Andersen et al., 2003), Sauer *et al.* (Sauer et al., 2005) and Nousiainen *et al.* (Nousiainen et al., 2006). We integrated the 114 proteins with confirmed centrosomal localization which Andersen *et al.* found by mass-spectrometry analysis of isolated human centrosomes (Andersen et al., 2003), with the 157 and 72 known spindle components, which Sauer *et al.* (Sauer et al., 2005) and Nousiainen *et al.* (Nousiainen et al., 2006) identified from purified human mitotic spindles, respectively, by mapping the given protein IDs to UniProt Accession Codes (UniProt ACs) (UniProt-Consortium, 2008). We also considered spindle proteins found in small-scale studies, by including the 80 proteins annotated with 'spindle' for 'cellular component' in GO (Ashburner et al., 2000), resulting in a final set of 308 non-redundant spindle proteins.

Exclusion of inaccessible sites

We assembled a set of template sequences from structures in the PDB (Berman et al., 2000) solved by X-Ray crystallography with a resolution of ≤3.5Å or by nuclear magnetic resonance (NMR). We assigned domains to human spindle proteins using the hidden Markov model (HMM) profiles from Pfam 22 (Eddy, 1998; Finn et al., 2008), which are based on sequences of evolutionarily conserved domains and thus allow the identification of domains for which no structural information is available yet. For each domain that contained any notP motifs, we used BLASTP (Altschul et al., 1997) to find the best matching template sequence in the PDB based on sequence identity, considering only hits with at least 80% coverage and an E-value $\leq 10^{-4}$. We then cut out the template domain, computed its surface accessibility using NACCESS (Hubbard & Thornton, 1993) and mapped it to the given query domain via the Pfam HMM alignment of the two domains. Sites in which all four motif residues had an

accessibility above 10 (absolute total side chain value) were considered accessible. We excluded all phosphorylation sites inside domains, except those which were deemed accessible or phosphorylated *in vivo* (see below).

Motif conservation based on motif presence

From all vertebrate orthologs provided by Ensembl 49 (Flicek et al., 2008), we chose those with a length within ±5% of the human substrate candidate in order to ensure comparability of relative positions. For a given human candidate protein, we identified all notP motif hits in each ortholog and computed their relative position (with respect to the length of the protein). A candidate site was considered conserved if at least 90% of the orthologs also contained a hit to the motif in about the same relative position (±1%).

Integration of* In vivo *phosphorylation data

We integrated the set of 736 *in vivo* phosphorylation sites in 260 proteins, which Nousiainen *et al.* identified from purified human mitotic spindles (Nousiainen et al., 2006), and the list of 16,989 *in vivo* phosphorylation sites in 3,181 proteins which Dephoure *et al.* extracted from lysates of M-phase arrested cells (Dephoure et al., 2008). Then, we mapped the given protein IDs to UniProt ACs (UniProt-Consortium, 2008) and checked for occurrence of the respective phosphopeptide, identified by tandem mass spectrometry, at about the same position (maximal offset of 20 residues) in the UniProt protein sequence. This resulted in a non-redundant set of 16,316 *in vivo* phosphorylation sites in 3,890 proteins.

cDNA constructs

FLAG-tagged full length sequences of human TPX2 (Q9ULWO), DYNLL1 (P63167), APC7 (Q9UJX3), MAP7 (Q14244), RACGAP1 (Q9H0H5), SPIN1 (Q9Y657), and NUSAP1 transcript variant 1 (NM_016359.2) (identical to 216-441 NUSAP1 Q9BXS6) inserted into pCMV6 entry vector were obtained from Origene. GST-tagged full length sequences of CETN1 (Q12798), YWHAG (P61981), YWHAE (P62258), DYNC1LI1 (Q9Y6G9), TBB4 (P04350), TUBG1 (P23258) and DYNLL1 (P63167) inserted in a pOPINJ vector were obtained from the cloning facility of the Centrosome 3D Consortium (M. Coll; IRB Barcelona). His-AurB clone was prepared by PCR, amplifying the cDNA from a pGEX-4T-1 construct (present from E. Conti; MPI) and

inserted into a pET28a vector. To obtain the EGFP version of hAurA, hAurA sequence was PCR amplified from a hAurA-pET28a clone (Bayliss et al., 2003) and inserted into a pHAT2-EGFP vector (Sardon et al., 2008).

Protein expression and purification

Aurora A and B proteins were expressed from pET28a-hAurA, pHAT2-EGFP-hAurA and pET28a-hAurB in *E. coli* and purified through their His tag as previously described (Bayliss et al., 2003). To express the different substrate candidates, HEK293 cells were transfected with the DNA constructs following the FuGENE6 protocol (Roche). After 48 hours, cells were collected by trypsinization, incubated with lysis buffer (50 mM Tris/HCl pH 7.4, 100 mM NaCl, 50 mM NaF, 1% Triton X-100, 1 mM EDTA, 1 mM EGTA, 1 mM DTT and protease inhibitors) on ice for 30 min and spun down (16,000 g) for 20 min at 4°C. Protein expression was checked in the supernatant fractions by western blotting. FLAG-tagged recombinant proteins were purified from the cell lysates by immunoprecipitation with anti-FLAG-M2 agarose (Sigma). After incubating the agarose beads in the lysate for 1 h, beads were washed twice with lysis buffer, twice with PBS-NaCl (PBS, 0.1 % triton X-100, 0.5 M NaCl) and twice with MOPS kinase buffer (50 mM MOPS pH 7.4, 5 mM $MgCl_2$, 1 mM EGTA, 1 mM EDTA, 10 mM β-glycerophosphate). To purify the GST-tagged proteins, Glutathione Sepharose 4B (Amersham) aliquots were incubated in the cell lysates for 1 h, washed twice with lysis buffer, twice with PBS-NaCl (PBS, 0.1 % triton X-100, 0.5 M NaCl) and twice with MOPS kinase buffer.

In Vitro *kinase assays*

Directly after protein purification, aliquots of beads covered with the candidate proteins were resuspended in 10 μl MOPS kinase buffer mixed with hAurA (0.2 μM), hAurB (1 μM) or buffer (to reduce the autophosphorylation signal from the kinases, both hAurA and hAurB were preincubated with 100 μM cold ATP at 37°C for 30 min before mixing with the candidate substrates). ^{32}P-ATP was then added to the reaction and samples were incubated at 37°C for 40 min. Reaction was stopped by adding SDS-page loading buffer, and proteins were separated by electrophoresis. The Coomassie-stained gels were scanned with the Odyssey imaging system (Li-cor). Autoradiographs were obtained by exposing the gel to a PhosphoImager film (Fuji-

Film) that was later scanned with a Typhoon Trio Imager (Amersham Biosciences). The intensity of the bands of the autoradiography was measured using ImageQuant 5.2 software. In parallel, the amount of protein loaded for each sample was determined by quantifying the Coomassie Brilliant Blue intensity with Odyssey software using different amounts of bovine serum albumin as standards. Since the amount of purified protein and the signal intensities varied widely in each case, the time of gel exposure to obtain the autoradiographies, shown in Figure 2, was adapted to each protein to get the best resolution, and thus the phosphorylation levels between different substrates cannot be readily compared in this figure. To carry out this comparison, we quantified the ^{32}P incorporation between the different samples of the same autoradiography and normalized the measurements by the μg of substrate protein present in the gel. When testing YWHAG and YWHAE, to avoid the interference of AurA autophosphorylation signal in the autoradiography (as the kinase and these substrates run at similar positions in the gels), we repeated the kinase assay using another recombinant kinase with a larger tag (GFP-AurA) and therefore running at a different position.

Due to the experimental procedure, the concentration of each substrate in the kinase assay varied in each experiment depending on its expression and immunoprecipitation efficiency. As an example, the substrate concentrations quantified from the experiment shown in Figure 2 were 372, 184, 36, 170, 322 and 106 ng/μl for GST-CENT1, GST-DYNC1LI1, GST-TBB4, GST-TUBG1, GST-TACC3 and GST-DYNLL1 respectively, and 4, 200, 40, 42, 74, 20 and 10 ng/μl for FLAG-TPX2, FLAG-DYNLL1, FLAG-MAP7, FLAG-APC7, FLAG-SPINDL1, FLAG-NUSAP and FLAG-RACGAP1, respectively.

The specific activity of the recombinant Aurora A and Aurora B used in these assays (determined using Histone H3 as standard substrate) is 0.071 μmol ATP x min^{-1} x mg^{-1} and 0.004 μmol ATP x min^{-1}x mg^{-1}, respectively.

Immunoprecipitation of FLAG-APC7 and FLAG-NUSAP for MS/MS analysis

FLAG-APC7 was expressed in HEK293 cells for 48 h and immunopurified as described above. Aliquots of beads binding the protein were resuspended in MOPS

kinase buffer in the presence and absence of Aurora A, and incubated with cold ATP during 40 min at 30°C. Reaction was stopped with SDS loading buffer.

HeLa cells were transfected with pCMV6-NUSAP1. To prepare an interphase cell lysate, cells were exponentially grown until confluency was reached. Cells were then trypsinized and lysed with lysis buffer (see above). To prepare mitotic cell lysates, transfected cells were first treated with thymidine 2mM for 16 hours, washed and released from the thymidine block for 8 hours, and then synchronized with nocodazole 2 μM for 16 hours. Mitotic cells were then shacked off and collected in a falcon tube. Nocodazole was removed and washed by spinning, and cells were incubated in DMEM with monastrol 100 μM in the absence or presence of MLN8237 (Selleck Chemicals) 0.5 μM or ZM447439 (Ditchfield et al., 2003) 2 μM for 1 hour. At the concentration used, MLN8237 totally inhibited Aurora A and only partially inhibited Aurora B (Suppl. Fig. 4). ZM447439 2 μM specifically inhibited Aurora B (Suppl. Fig. 4). After that, cells were spun down and lysed. NUSAP was immunoprecipitated from its FLAG tag as described above and loaded onto an SDS gel.

Mass spectrometry analysis

APC7 treated with buffer of hAurA or NUSAP1 directly isolated from cell lysates were hereafter separated by 1D-gel electrophoresis and excised bands were reduced, alkylated and trypsinized (Promega, Madison, WI, USA) following a previously described protocol (Shevchenko et al. 2006). Extracted peptides were analyzed by reversed phase liquid chromatography (Agilent 1200 nano flow pump, Agilent Technologies, CA or EasyLC, Proxeon A/S, Denmark) coupled to a mass spectrometer (Orbitrap XL or Orbitrap Velos, ThermoFisher, Bremen, Germany). MS/MS data were extracted and searched against the IPI Human database using Mascot version 2.2 (Matrix Science Inc., London, UK). 10 ppm was used as search accuracy for precursor ions where 0.5 Da and 20 mDa were used for MS/MS data, recorded in CID and HCD mode, respectively. N-terminal acetylation, oxidation of methionine and phosphorylation of serine, threonine and tyrosine residues were allowed as variable modifications. All cysteines were treated as being carbamidomethylated. To identify phosphorylation events specific to the hAurA

kinase, a label-free approach was chosen as previously described (Steen et al. 2005). In short: Extracted ion chromatograms (5ppm window) were created for the identified phosphopeptides for both treated and control samples. These chromatograms were compared to the chromatograms of (i) the corresponding unmodified peptide sequence and (ii) peptides not expected to be modified. The latter peptides serve as "loading control". Extracted ion chromatograms for the phosphopeptides, corresponding non-phosphorylated peptides and reference peptides are shown in Supp. Fig. 2. By comparing extracted ion chromatograms of the corresponding non-phosphorylated peptides in treated and control samples and using peptides not expected to be modified, we estimated the degree of phosphorylation. In Fig. 4A and 4B, the histograms show ratios based on the signal area of peptides carrying the phosphorylated NUSAP S240 compared to the signal areas of all matched peptides containing this residue.

Fluorescence Activated Cell Sorting (FACS)

FACS analyses were performed on a BD FACScan Flow Cytometer (BD Biosciences). As for the MS/MS analysis, Hela cells were blocked in G1 with thymidine 2 mM for 16 h, released in fresh DMEM for 7 h, and blocked in G2/M with nocodazole 2 μM for 16 h. Mitotic cells were then shaked off, washed with cold PBS and incubated with DMEM containing monastrol in the presence or absence of MLN8237 0,5 μM or ZM447439 2 μM for 1 h. In parallel, exponentially growing cells were grown to confluency and collected by trypsinization. All the collected cells were washed with PBS and fixed overnight in EtOH (-20°C). After washing with PBS, cells were stained with a propidium iodide solution (PI; 15 μg/mL)/ RNase A (30 μg/mL) overnight at 4°C.

Immunofluorescence analysis

HeLa cells grown on glass cover-slips were synchronized in mitosis as described above, and then incubated with monastrol (100 μM) in the absence or presence of MLN8237 (0,5 μM) or ZM447439 (2 μM) for 2 hours. Cells were fixed in ice-cold methanol and processed for immunofluorescence microscopy with anti-phospho-Aurora A (Cell Signaling C39D8) and anti-γ-tubulin antibodies (Sigma GT-88). DNA was stained with Hoechst 33342. Cells were observed on a Leica DMI6000B

microscope with the HCXPL APOCS 100x 1.4 objective. Images were taken with a Leica DFC 350FX camera, controlled by the LAS-AF6000 software. The phospho-Aurora A signal intensity at the center of the monopolar asters was measured with ImageJ.

Western Blots

Hela cells were synchronized in mitosis as described above. Mitotic cells were shaken off, incubated with monastrol (100 μM) in the absence or presence of MLN8237 (0,5 μM) or ZM447439 (2 μM) for 1 hour and lysed in lysis buffer (see above). 50 μg of cell extract per lane (as determined by Bradford assay, Bio-Rad protein assay) were loaded on SDS-PAGE, transferred to a nitrocellulose membrane and blotted with anti-phopho-Histone H3 (Upstate) and anti-α-tubulin antibodies (Sigma, DM1A).

References

Altschul, S.F., Madden, T.L., Schaffer, A.A., Zhang, J., Zhang, Z., Miller, W. & Lipman, D.J. (1997) Gapped BLAST and PSI-BLAST: a new generation of protein database search programs. *Nucleic Acids Res*, **25**, 3389-3402.

Andersen, J.S., Wilkinson, C.J., Mayor, T., Mortensen, P., Nigg, E.A. & Mann, M. (2003) Proteomic characterization of the human centrosome by protein correlation profiling. *Nature*, **426**, 570-574.

Ashburner, M., et al. (2000) Gene ontology: tool for the unification of biology. The Gene Ontology Consortium. *Nat Genet*, **25**, 25-29.

Bayliss, R., Sardon, T., Vernos, I. & Conti, E. (2003) Structural basis of Aurora-A activation by TPX2 at the mitotic spindle. *Mol Cell*, **12**, 851-862.

Berman, H.M., Westbrook, J., Feng, Z., Gilliland, G., Bhat, T.N., Weissig, H., Shindyalov, I.N. & Bourne, P.E. (2000) The Protein Data Bank. *Nucleic Acids Res*, **28**, 235-242.

Chatr-aryamontri, A., Ceol, A., Palazzi, L.M., Nardelli, G., Schneider, M.V., Castagnoli, L. & Cesareni, G. (2007) MINT: the Molecular INTeraction database. *Nucleic Acids Res*, **35**, D572-574.

Dephoure, N., Zhou, C., Villen, J., Beausoleil, S.A., Bakalarski, C.E., Elledge, S.J. & Gygi, S.P. (2008) A quantitative atlas of mitotic phosphorylation. *Proc Natl Acad Sci U S A*, **105**, 10762-10767.

Ditchfield, C., Johnson, V.L., Tighe, A., Ellston, R., Haworth, C., Johnson, T., Mortlock, A., Keen, N. & Taylor, S.S. (2003) Aurora B couples chromosome alignment with anaphase by targeting BubR1, Mad2, and Cenp-E to kinetochores. *J Cell Biol*, **161**, 267-280.

Eddy, S.R. (1998) Profile hidden Markov models. *Bioinformatics*, **14**, 755-763.

Finn, R.D., et al. (2008) The Pfam protein families database. *Nucleic Acids Res*, **36**, D281-288.

Flicek, P., et al. (2008) Ensembl 2008. *Nucleic Acids Res*, **36**, D707-714.

Hubbard, S.J. & Thornton, J.M. (1993) NACCESS. London, p. Computer Program.

Kerrien, S., et al. (2007) IntAct--open source resource for molecular interaction data. *Nucleic Acids Res*, **35**, D561-565.

Mishra, G.R., et al. (2006) Human protein reference database--2006 update. *Nucleic Acids Res*, **34**, D411-414.

Nousiainen, M., Sillje, H.H., Sauer, G., Nigg, E.A. & Korner, R. (2006) Phosphoproteome analysis of the human mitotic spindle. *Proc Natl Acad Sci U S A*, **103**, 5391-5396.

Sardon, T., Peset, I., Petrova, B. & Vernos, I. (2008) Dissecting the role of Aurora A during spindle assembly. *Embo J*, **27**, 2567-2579.

Sauer, G., Korner, R., Hanisch, A., Ries, A., Nigg, E.A. & Sillje, H.H. (2005) Proteome analysis of the human mitotic spindle. *Mol Cell Proteomics*, **4**, 35-43.

UniProt-Consortium. (2008) The universal protein resource (UniProt). *Nucleic Acids Res*, **36**, D190-195.

Wallace, I.M., O'Sullivan, O., Higgins, D.G. & Notredame, C. (2006) M-Coffee: combining multiple sequence alignment methods with T-Coffee. *Nucleic Acids Res*, **34**, 1692-1699.

Table and figure legends

Supp. Table 1: *Expression and interaction of known substrates.*

This table contains all the data used during the computational analyses, split in different tabs for clarity:

GO annotations: GO terms for cellular component and biological process for all 308 spindle proteins.

In vivo phosphorylation: Data for all spindle proteins that have been observed phosphorylated *in vivo*, derived from Nousiainen *et al.*, PNAS 2006 and Dephoure *et al.*, PNAS 2008.

Interaction with Aurora A: List of proteins in the spindle dataset that interact with Aurora A, either directly or mediated by a third protein (indirect interaction).

Conservation of known ph.sites: Shows the conservation of known Aurora A phosphorylation sites as computed by the BLAST-based and the presence-based method, respectively. Both methods were developed for this study and are described in the main text of the manuscript.

Alternative protein names: UniProt AC and ID as well as other common names for the 308 spindle proteins used in this study. Well-established Aurora substrates are highlighted in violet, experimentally tested potential target proteins in gray, and validated substrates in green.

Supp. Figure 1: *Filtering and ranking of known Aurora substrates.*
Proteins known to be phosphorylated by Aurora A or B, sorted by whether they contain a motif match (filter 1), localise to the spindle and/or centrosome (filter 2), whether motif hits are accessible (filter 3), and whether the proteins either contain conserved hits or interact with Aurora A (filter 4), and their position in the candidate ranking, if applicable.

Supp. Figure 2: *Normalization controls for the MS analysis of the APC7 phosphorylation at S85 by Aurora A.*

MS spectra (upper panels) and extracted ion chromatograms (control, mid panels vs. treatment, lower panels) are shown for A) the phosphorylated peptide: $VRP^{85}S_{phos}TGNSASTPQSQCLPSEIEVK^{3+}$, B) the corresponding non-phosphorylated peptide and C-E) selected tryptic APC7 peptides (AYAFVHTGDNSR $^{2+}$, AIQLNSNSVQALLLK $^{2+}$ and LFESVLPPLPAALQSR $^{2+}$, respectively) not expected to undergo modification and therefore used for normalization ("loading control"). As seen in panel A, the ion assigned to the phosphorylated peptide, $VRP^{85}S_{phos}TGNSASTPQSQCLPSEIEVK$ is not present in measurable amount in the control sample. This is in sharp contrast to the treated sample, where a clear signal is observed. This should be seen in reference to the signals of the un-modified peptide in the control and the treated samples (panel B) together with the loading controls (panels C through E). We were not able to measure a significant decrease of the non-phosphorylated peptide (panel B) in the treated sample and conclude that, though we have clear evidence for a kinase specific phosphorylation of serine 85, the level of this phosphorylation is low.

Supp. Figure 3: *Cell cycle status of Hela cells used in the MS/MS analysis.*

DNA profiles of confluent HeLa cells (A) and cells synchronized in mitosis by a thymidine block followed by a nocodazole (Noc) block (B-E). Samples C-E were subsequently incubated with monastrol 100 μM (Mon) in the absence (C) or presence of MLN8237 0,5 μM (D) or ZM447439 2 μM (E). The cell cycle status was evaluated by flow cytometry. 2n and 4n reflect relative DNA content and represent diploid (interphase) and tetraploid (mitotic) cells, respectively.

Supp. Figure 4: *Selectivity of MLN8237 and ZM447439 towards Aurora A and B.*

(A) The activity of Aurora A was calculated as the phospho-T288-Aurora A immunofluorescence signal measured at the center of monopolar asters formed in Hela cells treated with monastrol in the absence (Control) or presence of MLN8237 0,5 μM (MLN) or ZM447439 2 μM (ZM). Pictures (left) show representative images of the mitotic structures formed in each condition. The bar graph (right) represents the calculated fluorescence intensity as a percentage of the control signal. (B) Aurora B

activity, determined as phospho-S10-Histone H3 signal by Western blot (anti-pHH3), was measured in cell lysates obtained from mitotic cells incubated with monastrol in the absence (Control) or presence of MLN8237 0,5 μM (MLN) or ZM447439 2 μM (ZM). α-Tubulin (anti-αTub) levels were used as loading controls. The bar graph (right) shows the calculated pHH3 signal normalized by the α-tubulin signal, as a percentage of the control sample.

Substrate	Kinase	Filter 1:	Filter 2:	Filter 3:	Filter 4:	Rank
TPX2 (Q9ULW0)	A					3
INCE (Q9NQS7)	B					4
AURKB (Q96GD4)	B					6
PLK1 (P53350)	A					7
CND1 (Q15021)	B					15
TOP2A (P11388)	B					19
RGAP1 (Q9H0H5)	B					20
NIN (Q8N4C6)	A					32
KNTC2 (O14777)	B					44
CND2 (Q15003)	A					45
KIF23 (Q02241)	B					47
STK6 (O14965)	A					54
KC1A (P48729)	A					79
BIRC5 (O15392)	B					-
DLG7 (Q15398)	A					-
KIF2A (O00139)	A/B					-
KIF2C (Q99661)	B					-
LATS2 (Q9NRM7)	A					-
MAP9 (Q49MG5)	A					-
NDEL1 (Q9GZM8)	A					-
RASF1 (Q9NS23)	A					-
BRCA1 (P38398)	A					-
CENPA (P49450)	A/B					-
CPEB1 (Q9BZB8)	A					-
DESM (P17661)	B					-
FOS (P01100)	A					-
GFAP (P14136)	B					-
H31 (P68431)	A/B					-
H33 (P84243)	A/B					-
IKBA (P25963)	A					-
MBD3 (O95983)	A					-
MPIP2 (P30305)	A					-
P53 (P04637)	A					-
RALA (P11233)	A					-
TACC3 (Q9Y6A5)	A					-
VIME (P08670)	A/B					-

Supp Figure 1

Supplementary Figure 2

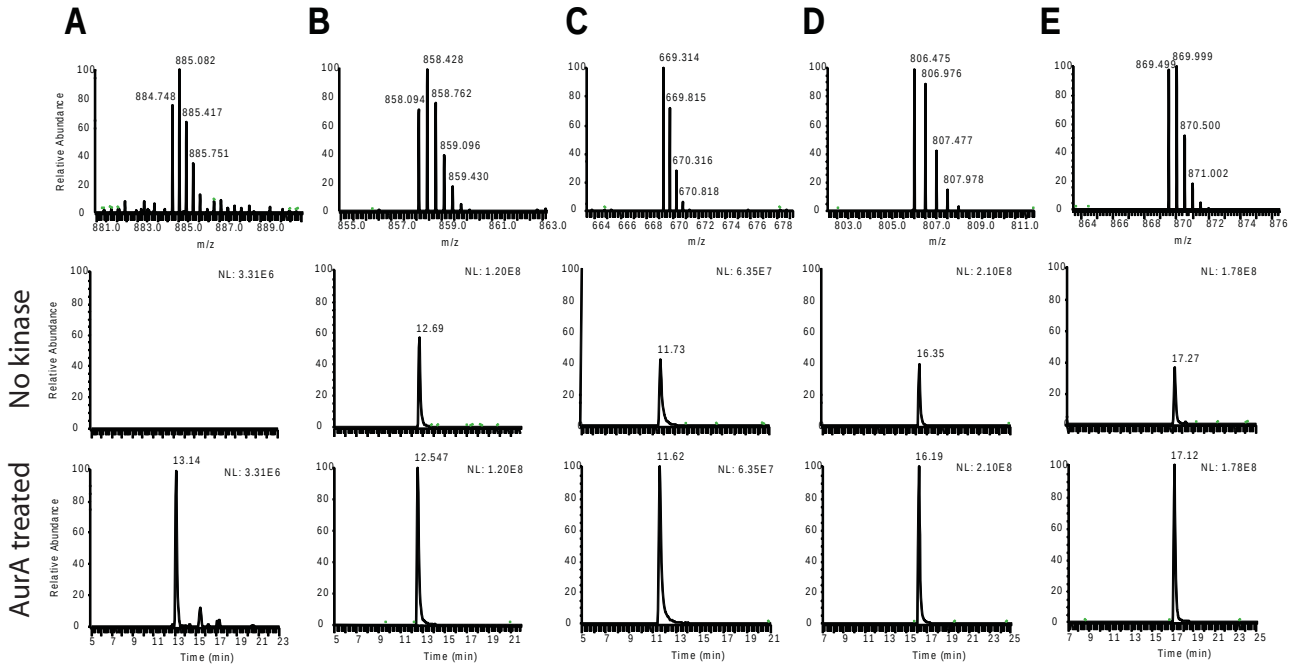

Supplementary Figure 3

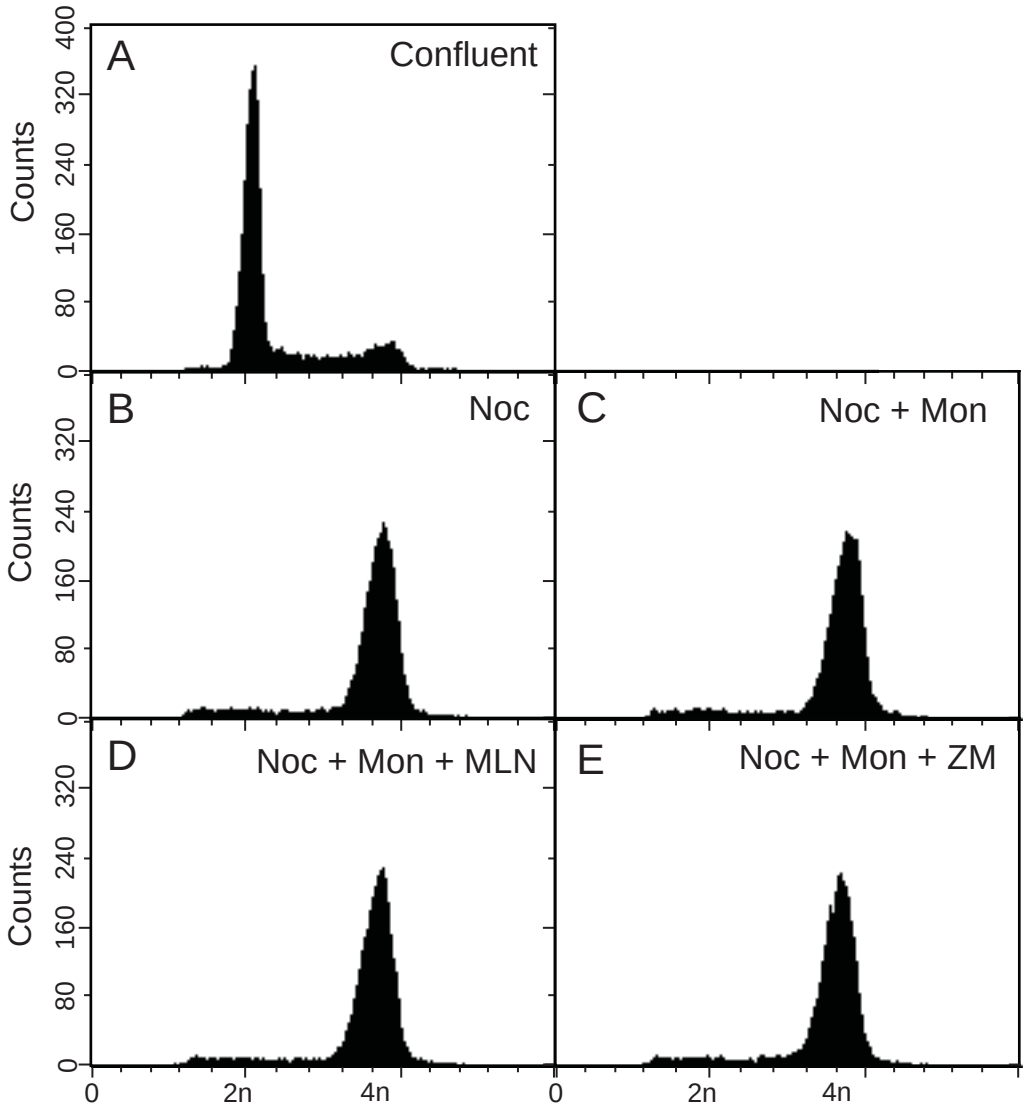

	<2n (%)	2n (%)	2n<x< 4n (%)	4n (%)
A	1,0	72,1	12,8	14,1
B	2,8	3,2	5,3	87,4
C	2,5	3,2	4,7	87,3
D	2,9	3,0	6,7	86,4
E	2,7	3,0	7,6	86,1

Supplementary Figure 4

A

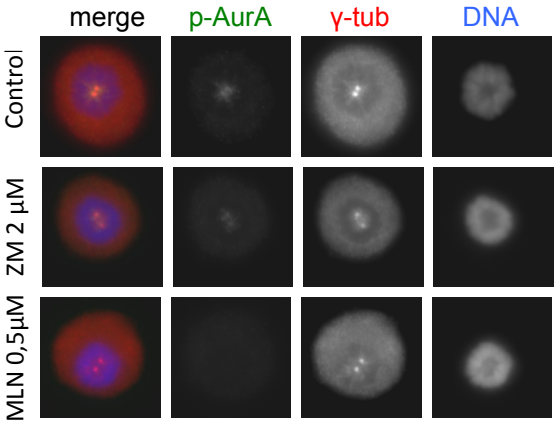

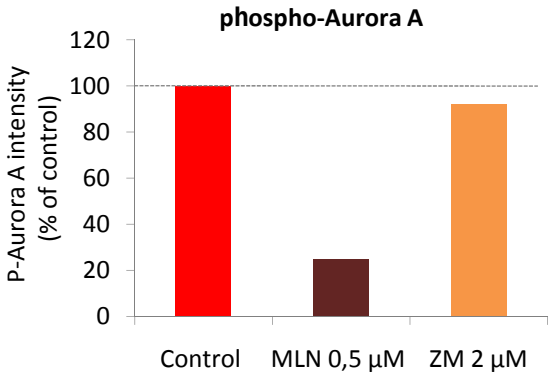

B